Carbonic Anhydrase Models. 5. Tris(4,5-di-*n*-propyl-2-imidazolyl)phosphine–Zinc(2+) and Bis(4,5-diisopropyl-2-imidazolyl)-2-imidazolylphosphine–Zinc(2+). Catalysts Facilitating $HCO_3^- \rightleftharpoons CO_2$ Interconversion

H. Slebocka-Tilk, J. L. Cocho, Z. Frakman, and R. S. Brown*

Contribution from the Department of Chemistry, University of Alberta, Edmonton, Alberta, Canada T6G 2G2. *Received July 22, 1983*

Abstract: The title trisimidazolylphosphines (**4a** and **5**, respectively) were prepared and their Zn^{2+} and Co^{2+} complexes studied as active-site models for carbonic anhydrase. Both ligands bind Zn^{2+} more strongly than they do Co^{2+}. NMR studies show that **4a**·$ZnCl_2$ exists as a 1:1 complex which undergoes dynamic exchange on the NMR time scale indicative of an imidazole debinding, tautomerization, and rebinding through the opposite nitrogen. **5**·$Zn^{2+}Cl_2^-$ exists as a nonexchanging 1:1 complex, but if ClO_4^- is used as a counterion, an exchange phenomenon is indicated. While **4a**·Co(II) shows some minor tendency to adopt a tetrahedral "blue" complex, **5**·Co(II) forms definite 4- or 5-coordinate chelates whose visible absorption spectra are dependent upon the presence of added anions. However, if ClO_4^- or NO_3^- are used as counterions, the spectrum of **5**·Co(II) shows little evidence for 4- or 5-coordination. Catalytically both **4a**·Zn^{2+} and **5**·Zn^{2+} enhance the rate of attainment of $HCO_3^- \rightleftharpoons CO_2$ equilibrium, with the latter being most active. Catalysis in both cases is inhibited by the presence of monovalent anions, and for both complexes a saturation in the rate of $HCO_3^- \rightleftharpoons CO_2$ equilibration is seen as a function of increasing [$NaHCO_3$]. Initial rate experiments were attempted but are shown to be problematic under the conditions required for the study.

Carbonic anhydrase (CA) is a widely occurring Zn^{2+} metalloenzyme found in virtually every living system. Although its only known physiological purpose involves catalyzing the deceptively simple process shown in eq 1, it plays a key role in such diverse

$$H^+ + HCO_3^- \rightleftharpoons H_2O + CO_2 \qquad (1)$$

processes as pH control, photosynthesis, gas balance, and calcification or shell formation.[1] In addition to its widespread occurrence, it is a worthy entity for study from a catalytic standpoint since its turnover numbers are among the highest for any known enzyme. In view of the above, some time ago we embarked on a program to synthesize and study small metal-binding ligands designed to approximate the active-site region that has been shown by X-ray crystallographic techniques to consist of an essential Zn^{2+} ion bound to the protein matrix in a low-coordinate distorted tetrahedral fashion by three histidine imidazole units.[2] As a result of these studies it appeared that reasonable models such as **1** and **2** could be constructed which when bound to M^{2+} in a tridentate manner exhibited structural[3a,b] and spectroscopic[3c] properties in common with CA, as well as the ability to catalyze the interconversion of HCO_3^- and CO_2. One of these, **2**–Co(II), provided a simple model which approximated in a reasonable way the visible absorption properties of Co(II)–CA in terms of the shift in spectroscopic pK_a to higher values in the presence of monovalent anions.[3c] However, like all simple systems which have been studied as models for CA,[4] **1c**–Zn^{2+} and **2**–Zn^{2+} are only modest catalysts at best for the hydration of CO_2. Hence our original expectation that the dominant consideration in creating efficient catalytic entities for $HCO_3^- \rightleftharpoons CO_2$ interconversion rests in providing a tridentate ligand capable of binding the requisite Zn^{2+} in a distorted, low-coordinate environment is apparently too simple.

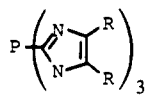

1 a R = H
b R = CH_3
c R = $CH(CH_3)_2$

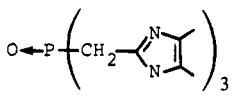

2

Since X-ray crystallographic analysis of the **1c**–Zn^{2+}–$2Cl^-$ complex indicated that the imidazole isopropyl groups formed a restrictive cavity such that only one additional ligand (Y = Cl^-) could be bound to the 4-coordinate Zn^{2+} ion[3b] as in **3a**, it seemed

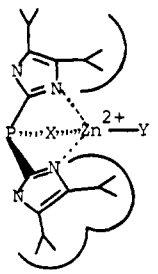

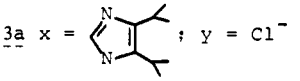

3a x = ; y = Cl^-

(1) For recent reviews of carbonic anhydrase see: (a) Lindskog, S.; Henderson, L. E.; Kannan, K. K.; Liljas, A.; Nyman, P. O.; Strandberg, B. "The Enzymes", Boyer, P. D., Ed.; Academic Press: New York, 1971; Vol. 5, pp 587–665. (b) Coleman, J. E. "Inorganic Biochemistry"; Eichorn, G. L., Ed.; Elsevier: 1973; Vol. 1, pp 488–548. (c) Dunn, M. F. *Struct. Bonding (Berlin)* **1975**, *23*, 61–122. (d) Pocker, Y.; Sarkanen, S. *Advan. Enzymol.* **1978**, *47*, 149–274. (e) Wyeth, P.; Prince, R. H. *Inorg. Perspect. Biol. Med.* **1977**, *1*, 37–71. (f) Prince, R. H. In "Advances in Organic Chemistry and Radiochemistry"; Emeléus, H. J., Sharpe, A. G., Eds.; Academic Press: New York, 1979; Vol. 2, pp 349–440. (g) "Biophysics and Physiology of Carbon Dioxide"; Bauer, C., Gros, G., Bartels, H., Eds.; Springer-Verlag: Berlin, 1980. (h) Hay, R. W. *Inorg. Chim. Acta* **1980**, *46*, L115–117. (i) Golding, B. T.; Leigh, G. J. *Inorg. Biochem.* **1979**, *1*, 50–55. (j) Galdes, A.; Hill, H. A. O. *Ibid.* **1979**, *1*, 317–355. (k) Bundy, H. F. *Comp. Biochem. Physiol. B* **1977**, *57*, 1–7. (l) Lindskog, S. In "Advances in Inorganic Biochemistry"; Eichhorn, G. L., Marzilli, L. G., Eds.; Elsevier: New York, 1982; pp 115–170.

(2) (a) Kannan, K. K.; Petef, M.; Cid-Dresdner, H.; Lövgren, S. *FEBS Lett.* **1977**, *73*, 115–119. (b) Notstrand, B.; Vaara, I.; Kannan, K. K. In "The Isozymes"; Markert, C. L., Ed.; Academic Press: New York, 1975; Vol. 1, pp 575–599. (c) Kannan, K. K.; Notstrand, B.; Fridborg, K.; Lövgren, S.; Ohlssen, A.; Petef, M. *Proc. Natl. Acad. Sci. U.S.A.* **1975**, *72*, 51–55. (d) Liljas, A. et al. *Nature (London), New Biol.* **1972**, *235*, 131–137. (e) Kannan, K. K. et al. *Cold Spring Harbor Symp. Quant. Biol.* **1971**, *36*, 221–231.

(3) (a) Brown, R. S.; Curtis, N. J.; Huguet, J. *J. Am. Chem. Soc.* **1981**, *103*, 6953–6959. (b) Read, R. J.; James, M. N. G. *Ibid.* **1981**, *103*, 6947–6952. (c) Brown, R. S.; Salmon, D.; Curtis, N. J.; Kusuma, S. *Ibid.* **1982**, *104*, 3188–3194.

(4) (a) Wooley, P. *Nature (London)* **1975**, *258*, 677–682. (b) Wooley, P. *J. Chem. Soc., Perkin Trans. 2* **1977**, 318–324. (c) Wooley, P. "Biophysics and Physiology of Carbon Dioxide"; Baur, C., Gros, G., Bartels, H., Eds.; Springer-Verlag: Berlin, 1980; pp 216–225. (d) Tabushi, I.; Kuroda, Y.; Mochizuki, A. *J. Am. Chem. Soc.* **1980**, *102*, 1152–1153. (e) Pocker, Y.; Meany, J. E. *Ibid.* **1967**, *89*, 631–636. (f) Chaffee, E.; Dasgupta, T. P.; Harris, G. M. *Ibid.* **1973**, *95*, 4169–4173. (g) Palmer, D. A.; Harris, G. M. *Inorg. Chem.* **1974**, *13*, 965–969. (h) Harrowfield, J. MacB.; Norris, V.; Sargeson, A. M. *J. Am. Chem. Soc.* **1976**, *98*, 7282–7289.

0002-7863/84/1506-2421$01.50/0

likely that one of the reasons for the low catalytic activity of **1c**–Zn^{2+} could reside in the inability of the complex to accommodate the increased coordination number (which would be required for ligand exchange during the catalytic cycle[3a]) without severe steric buttressing.

Therefore, a study was undertaken of ligands **4a**, **4b**, and **5**, each of which when bound to Zn^{2+} would provide a cavity with greater accessibility to the reagents and at the same time enforce a low (4 or 5) coordination environment. In addition, ligand **4b**

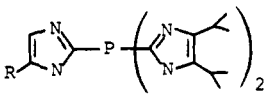

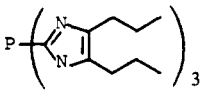

4a R = H
b R = CH_2CH_2OH

5

possesses a remote hydroxyethyl group that was introduced as an approximation of the active-site threonine OH group which has been invoked as being of assistance during the hydration of CO_2 by the enzyme.[2b] The following represents our findings during the course of this study.

Experimental Section

UV–visible absorption spectra were recorded with a Cary Model 210 spectrophotometer. Routine IR and ^1H NMR spectra were obtained with a Nicolet FTIR spectrophotometer and Bruker WP-80 spectrometer, respectively. Mass spectra were obtained with an MS-50 spectrometer. The effects of added Zn^{2+} on the ^1H NMR spectra of **4a** and **5** were determined on a Bruker WH-200 FT NMR spectrometer.

A. Syntheses. Bis(4,5-diisopropyl-2-imidazolyl)-2-imidazolylphosphine (4a). To a stirring solution of 16.88 g (0.0747 mol) of freshly distilled *N*-(dimethoxymethyl)-4,5-di-isopropylimidazole[5] in 150 mL of dry ether held at −40 °C was added via syringe 45.32 mL (0.0747 mol) of 1.65 N *n*-BuLi in hexane at such a rate that the temperature did not exceed −40 °C. After addition, the yellow solution was stirred an additional 20 min and then cooled to −60 °C. This solution was then transferred by syringe to a second flask containing a stirring solution of 5.13 g (0.0374 mol) of freshly distilled PCl_3 in 150 mL of dry THF also held at −60 °C. The rate of addition was adjusted so that the temperature in the second flask remained at less than −55 °C, and after addition, the mixture was allowed to slowly come to room temperature overnight while stirring. In the morning in a third flask was prepared the anion of *N*-(diethoxymethyl)imidazole[5] at −40 °C by the addition of 31.7 mL (0.523 mol) of 1.65 N *n*-BuLi to 8.9 g of the imidazole (0.0523 mol) in 150 mL of dry THF held at −40 °C. After this mixture was stirred for 20 min to ensure complete deprotonation, it was transferred via syringe to the flask containing chlorobis(*N*-(dimethoxymethyl)-4,5-diisopropyl-2-imidazolyl)-phosphine held at −40 °C. The resultant coral-colored mixture was allowed to come to room temperature and stirred over a weekend.

Workup of the product consisted of adding 150 mL of concentrated NH_4OH to the resultant mixture, separation of the organic layer, and rotary evaporation of the solvents. Meanwhile, the NH_4OH layer was extracted with 3 × 100 mL $CHCl_3$, and the combined $CHCl_3$ extracts were stripped of solvent, the residue being combined with that from the ether layer. Final deblocking was accomplished by refluxing the combined residues with 150 mL of 1:1 methanol–H_2O for 45 min. After the mixture was cooled, 7.0 g of yellow powder was filtered out and washed with ether to yield 4 g of crude product. Recrystallization was effected by dissolving this crude product in methanol and adding H_2O to turbidity. After refrigeration for 24 h, 3.6 g of pure product (24.1% overall yield) was obtained: mp 194–195 °C; ^1H NMR (CD_3OD) δ 1.2 (d of d, 24 H), 3.1 (m, 4 H), 7.1 (s, 2 H); IR (CCl_4 cast): 2899.1, 2869.7, 2596.9, 1237.8 cm^{-1}; mass spectrum, *m/z* calcd for $C_{21}H_{33}N_6P$, 400.2504; obsd, 400.2504. Anal. C, H, N.

Bis(4,5-diisopropyl-2-imidazolyl)-4(5)-(2-hydroxyethyl)-2-imidazolylphosphine (4b). This was prepared in a stepwise fashion in an analogous fashion to **4a**. In the first step, 16.6 g of *N*-(dimethoxymethyl)-4,5-diisopropylimidazole[5] in 150 mL of dry ether was converted to its 2-lithio derivative by treatment with 48.96 mL of 1.5 N *n*-BuLi. As before, it was added via syringe at −60 °C to 4.95 g (0.0367 mol) of distilled PCl_3 in 100 mL of dry THF at such a rate that the temperature in the second flask did not exceed −60 °C. After the mixture was stirred at room temperature overnight, this flask was again cooled to −40 °C in preparation for the next step.

Scheme I

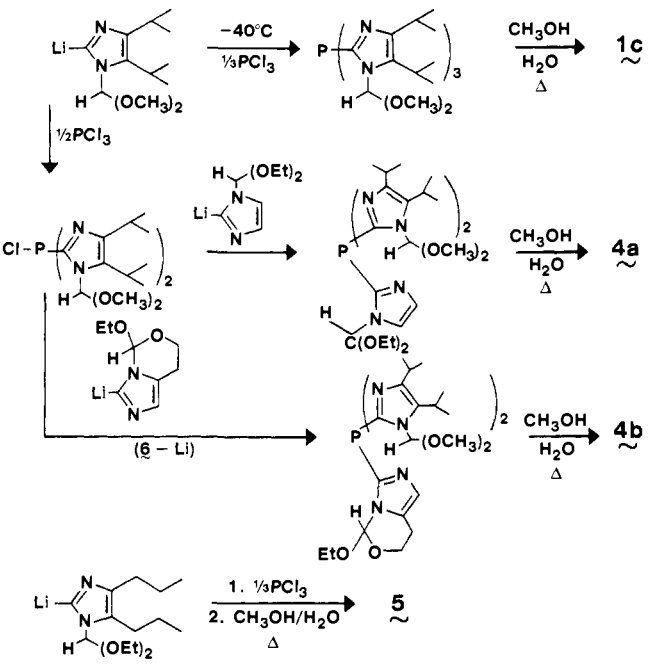

To 8.08 g (0.0481 mol) of the cyclic amide acetal of 4(5)-hydroxyethyl)imidazole[6] (**6**, Scheme I) in 100 mL of dry THF cooled to −40 °C was added 32.0 mL (0.0481 mol) of 1.5 N *n*-BuLi. The resultant red solution was stirred at −40 °C for an additional 20 min and then transferred by syringe to the first flask. The resultant mixture was allowed to come to room temperature overnight and yielded an orange-red suspension which was stirred an additional 24 h. Workup consisted of evaporating the solvent and addition of $CHCl_3$ and 100 mL of concentrated NH_4OH to dissolve the salts. The NH_4OH layer was extracted with $CHCl_3$, and the combined organic layers were washed with saturated NaCl. After rotary evaporation of the volatiles, the crude residue was refluxed with 100 mL of 1:1 methanol–H_2O to effect deprotection. Evaporation of the methanol produced a yellow solid which was filtered and after washing with ether yielded 6.5 g of white powder. Recrystallization from methanol/H_2O produced 3.5 g of white needles (21%): mp 187–188 °C after drying; ^1H NMR ($CDCl_3$) δ 1.25 (d, 24 H), 2.75–3.25 (m, 6 H), 3.87 (t, 2 H), 6.91 (s, 1 H); IR ($CHCl_3$ cast) 3126.6 (br), 2961, 2927, 2869, 1461, 1389, 1364, 1059 cm^{-1}; mass spectrum, *m/z* calcd for $C_{23}H_{37}N_6OP$, 444.2771; obsd, 444.2772. Anal. C, H, N.

Tris(4,5-di-*n*-propyl-2-imidazolyl)phosphine (5). *N*-(Diethoxymethyl)-4,5-di-*n*-propylimidazole. A mixture of 41.1 g (0.27 mol) of 4,5-di-*n*-propylimidazole,[7] 1 g of *p*-toluenesulfonic acid, 152 g of triethyl orthoformate, and 200 mL of toluene was heated at reflux until no further ethanol was distilled (~2 h). The remaining volatiles were removed under reduced pressure and 1 g of solid Na_2CO_3 was added to the residue. Vacuum distillation afforded 46.7 g (71%) of product as a yellow oil, bp 103–105 °C (0.4 torr); ^1H NMR ($CDCl_3$) δ 0.925 (t, 6 H), 1.21 (t, 6 H), 1.35–1.95 (m, 4 H), 2.3–3.25 (m, 4 H), 3.55 (q, 4 H), 5.91 (s, 1 H); 7.59 (s, 1 H); mass spectrum, *m/e* calcd for $C_{14}H_{26}N_2O_2$, 254.1994; obsd, 254.1992.

The phosphine was prepared according to a general procedure previously reported:[5] from 38.5 g (0.152 mol) of *N*-(diethoxymethyl)-4,5-di-*n*-propylimidazole converted to its 2-lithio anion at −40 °C by treatment with 92.5 mL (0.152 mol) of 1.6 N *n*-BuLi followed by the addition of 6.96 g (0.0506 mol) of freshly distilled PCl_3 was obtained after the usual workup procedure[5] and deblocking with 300 mL of 1:1 methanol–H_2O 6.1 g (25%) of tris(4,5-di-*n*-propyl-2-imidazolyl)phosphine after recrystallization from hexane: mp 156 °C; ^1H NMR ($CDCl_3$) δ 0.96 (t, 18 H), 1.65 (sextet, 12 H), 2.52 (t, 12 H); IR ($CHCl_3$ cast) 3500 (br), 3080, 2960, 2930, 2855, 1580, 1460, 1455, 1375, 1160 cm^{-1}; mass spectrum, *m/z* calcd for $C_{27}H_{45}N_6P$, 484.3443; obsd, 484.3447. Anal. C, H, N.

B. Ligand pK_a and pK_M^{2+} values were determined by potentiometric titration and the data analyzed as previously described[8] except for reasons of solubility a medium of 80% ethanol/H_2O (v/v) was used throughout.

(5) Curtis, N. J.; Brown, R. S. *J. Org. Chem.* **1980**, *45*, 4038–4040.
(6) Brown, R. S.; Ulan, J. G. *J. Am. Chem. Soc.* **1983**, *105*, 2382–2388.
(7) Bredereck, H.; Theiling, G. *Chem. Ber.* **1953**, *86*, 88–96.
(8) Brown, R. S.; Huguet, J. *Can. J. Chem.* **1980**, *58*, 889–901.

Table I. pK_a and pK_M^{2+} Values for Ligands Determined in 80% Ethanol/H_2O[a]

ligand	pK_{a_1}	pK_{a_2}	pK_{a_3}	$pK_{Zn^{2+}}$	$pK_{Co^{2+}}$
4a	1.8	3.52	6.67	8.7	7.7
4b	0.5	3.55	6.27	6.5	5.7
1c[b]	2.55	4.36	6.67	6.00	3.48
5	2.35	3.15	6.55	8.0	7.6

[a] Procedure as described in Experimental Section.[8] [b] Values from ref 3a.

pH values are those read from a Radiometer Model GK2322C combination electrode immersed directly in the solution. In order to correct for the highly organic nature of the medium, electrode standardization was accomplished as follows. A 0.117 N solution (titrated with NaOH) of $HClO_4$ with a total $\mu = 0.2$ M ($NaClO_4$) was prepared in 80% ethanol/water. By 100-fold dilution of a portion of this solution with 80% ethanol/water ($\mu \simeq 0.2$ M, $NaClO_4$) was prepared a second 1.17×10^{-4} N solution of $HClO_4$. After the electrode was equilibrated by soaking in the 0.117 N $HClO_4$ solution for ~30 min, standardization of the pH assembly was performed in the usual way by assuming the $HClO_4$ was completely dissociated and assigning the two stock solutions pH values of 0.93 and 3.93, respectively. Having completed the standardization in this way, a typical titration was performed with constant solvent composition and ionic strength as follows. A 5-mL solution of 80% ethanol/H_2O containing 0.025 mmol of ligand and 0.093 mmol of $HClO_4$, $\mu = 0.2$ M $NaClO_4$, was titrated with 0.2 N NaOH in 80% ethanol/H_2O under an atmosphere of N_2. To determine metal-binding constants the starting 5-mL solution contained 0.025 mmol of ligand, 0.140 mmol of $HClO_4$, 0.0124 mmol of M^{2+} $(ClO_4^-)_2$, $\mu = 0.2$ M $NaClO_4$. Metal solutions were standardized by EDTA titrations.[9] pK_a and pK_M^{2+} values reported in Table I are the averages of at least two determinations and have a precision of ±0.1 unit.

C. Kinetic determinations of the reaction rates for HCO_3^- dehydration or CO_2 hydration were performed on a Durrum–Gibson stopped-flow instrument thermostated at 25.0 ± 0.2 °C. Absorbance vs. time traces were digitally stored on a TDI Model 1024-C Transient recorder having 8-bit resolution. Data manipulations and calculations were performed by a Commodore/PET Model 4032 microcomputer interfaced into the system, and the k_{obsd} values reported are those calculated by fitting the absorbance/time data to a standard first-order exponential model via a nonlinear least-squares technique.[10] In general, the values obtained are the averages of six to ten determinations for a given set of conditions.

Since neither CO_2 nor HCO_3^- have easily monitored spectral properties, well-established indicator techniques[11] are used whereby the change in $[H^+]$ accompanying CO_2 hydration or HCO_3^- dehydration is monitored by observing the change in absorbance of an indicator anion (A^-) whose response to $\Delta[H^+]$ is rapid relative to the reaction in question (eq 2).

$$AH + HCO_3^- \overset{\text{fast}}{\rightleftharpoons} HCO_3^- + H^+ + A^- \underset{k_r}{\overset{k_f\ (\text{slow})}{\rightleftharpoons}} H_2O + CO_2 + A^- \tag{2}$$

Two pieces of kinetic data were obtained in this study. To obtain the first which is a measure of the rate of attainment of equilibrium, appropriate buffering conditions were employed (2.5×10^{-2} M HEPES) such that during the course of the reaction the pH change was <0.05 unit and the total Δabsorbance at 600 nm was ≳0.02 unit. Under these conditions, eq 2 reduces to a typical pseudo-first-order equilibrium reaction (eq 3), where the rate of change in $[HCO_3^-]$ or rate of change in

$$HCO_3^- \underset{k_r}{\overset{k_f}{\rightleftharpoons}} CO_2 \tag{3}$$

$[A^-]$ is given by eq 4 where X and X_e denote the concentration of the

$$-\frac{d[HCO_3^-]}{dt} = \frac{d[CO_2]}{dt} = \frac{d[A^-]}{dt} = k_{obsd}(X_e - X) = (k_f + k_r)(X_e - X) \tag{4}$$

product of the reaction (HCO_3^- for hydration and CO_2 for dehydration) at time t and equilibrium, respectively.[12] Thus, k_{obsd} is given by $(k_f + k_r)$, the sum of all the forward and reverse rate constants which includes those dependent on various forms of the buffer and other species present in the solution including the catalyst.

A typical experiment was performed as follows. Into one drive syringe was placed a solution consisting of 1×10^{-3} M indicator (bromocresol purple, BCP), 5×10^{-2} M HEPES adjusted to the desired pH by addition of 1 M NaOH, and the appropriate amount of $NaClO_4$ to bring the ionic strength to 0.2 M. The second drive syringe contained a solution of between 2×10^{-4} and 2.5×10^{-3} M $NaHCO_3$ brought to an ionic strength of 0.2 M with $NaClO_4$. The solvents in both syringes consisted of 80% (v/v) ethanol/H_2O. After rapid mixing of equal volumes of both solutions at 25 °C, reaction rates were monitored by observing the change in $[BCP^-]$ at 600 ± 20 nm. Control experiments in which no $NaHCO_3$ was added to the second syringe showed no change in $[BCP^-]$ after the initial rapid mixing, indicating that the various acid–base equilibria were established rapidly relative to the slower reaction in question.

In order to assess the effect of added catalyst on k_{obsd}, solutions identical with those above were used except that between 5 and 20×10^{-4} M each of **4a**, **4b**, or **5** and $Zn(ClO_4)_2$ was introduced into the buffer-containing syringe. Catalyst solutions were used immediately after preparation since they exhibit diminished activity on standing for prolonged periods. Values of k_{cat}^{obsd}, the second-order catalytic rate constant, were obtained as in eq 5 where k'_{obsd} and k_{obsd} refer to the pseudo-first-

$$k_{cat}^{obsd} = \frac{k'_{obsd} - k_{obsd}}{[CAT]} \tag{5}$$

order rate constants observed in the presence and absence of added catalyst, and [CAT] is taken to be that in syringe 1 corrected for a dilution factor of 2 on mixing.

In order to obtain the forward rate constant (k_f) as in eq 3, initial rate experiments were undertaken in which the reaction was monitored from the direction of $HCO_3^- + H^+ \rightarrow$ dehydration for the first few percent.[11] From eq 6, the rate of disappearance of HCO_3^- (or rate of appearance

$$\frac{-d[HCO_3^-]}{dt} = \frac{-d[H^+]}{dt} = \frac{d[A^-]}{dt} = \frac{d(ABS_{600})}{dt}\frac{d[H^+]}{d(ABS_{600})} \tag{6}$$

of indicator anion) can be expressed in terms of measurable quantities obtained under the experimental conditions. $d(ABS_{600})/dt$ is simply the rate of change in measured absorbance at 600 nm while the second term $d[H^+]/d(ABS_{600})$ is an experimental buffer factor relating the changes in absorbance to changes in $[H^+]$.[11] In aqueous solutions buffer factors can be calculated as in previous studies[11] if one knows exactly the pK's of the buffer and indicator and has knowledge of the change in molar extinction coefficient between acidic and basic forms of the indicator. However, since the solutions required here for catalyst solubility are highly organic in nature, it is more accurate to determine the buffer factors under the experimental conditions by rapidly mixing the buffered pH 6.4–6.5 indicator solution and a second solution containing a known $[HClO_4]$ in 80% ethanol/H_2O ($\mu = 0.2$ M $NaClO_4$) and then determining the absorbance change. Since the [buffer] exceeds the added $[HClO_4]$ by a factor of at least 50, the changes in measured pH are minimal, amounting to at most 0.05 unit. Typically at pH 6.5, the addition of a solution of 6.6×10^{-4} M $[HClO_4]$ to one containing 5×10^{-2} M HEPES and 1×10^{-3} M BCP gives absorbance changes of ~0.02 unit at 600 nm. Plots of $\Delta[H^+]$ against $\Delta(ABS_{600})$ are linear over values of $1 \times 10^{-4} - 1 \times 10^{-3}$ M in added $[H^+]$, the slope being the experimental buffer factor. Initial rates were then determined under the identical[11h] conditions by measuring the rate of change in absorbance at 600 nm over the first 5% of the dehydration reaction in a zero-order fashion. Evaluation of the initial rate constant (k_f) is given by eq 7 where $[NaHCO_3]_i$

$$k_f = \frac{[d(ABS_{600})/dt][d[H^+]/d(ABS_{600})]}{[NaHCO_3]_i} \tag{7}$$

(9) Flaschka, H. A. "EDTA Titrations", 2nd ed.; Pergamon Press: New York, 1964.

(10) We thank Dr. J. M. Buschek for adapting a nonlinear least-square program for use on this microprocessor.

(11) (a) Khalifah, R. G. *J. Biol. Chem.* **1971**, *246*, 2561–2573. (b) Kernohan, J. C. *Biochim. Biophys. Acta* **1965**, *96*, 304–317. (c) Gibbons, B. H.; Edsall, J. T. *J. Biol. Chem.* **1963**, *238*, 3502–3507. (d) Ho, C.; Sturtevant, J. M. *Ibid.* **1963**, *238*, 3499–3501. (e) Khalifah, R. G.; Edsall, J. T. *Proc. Natl. Acad. Sci. U.S.A.* **1972**, *69*, 172–176. (f) DeVoe, H.; Kistiakowsky, G. B. *J. Am. Chem. Soc.* **1961**, *83*, 274–279. (g) Pocker, Y.; Diets, T. L. *Ibid.* **1982**, *104*, 2424–2435. Pocker, Y.; Diets, T. L. *Ibid.* **1983**, *105*, 980–986. (h) "Identical" conditions can of course not be exactly employed to quantitatively relate the experimental buffer factor with absorbance changes occurring during HCO_3^- dehydration since the latter experiment requires the presence of $NaHCO_3$ while the former does not. We believe, as discussed subsequent in the text, that the bromocresol purple indicator used here associates with both $Na^+HCO_3^-$ and catalyst to form a "new" ternary indicator–solute complex whose response to $\Delta[H^+]$ differs from that of BCP determined in the absence of $NaHCO_3$.

(12) Jencks, W. P. "Catalysis in Chemistry and Enzymology"; McGraw-Hill: New York, 1969; pp 586–589.

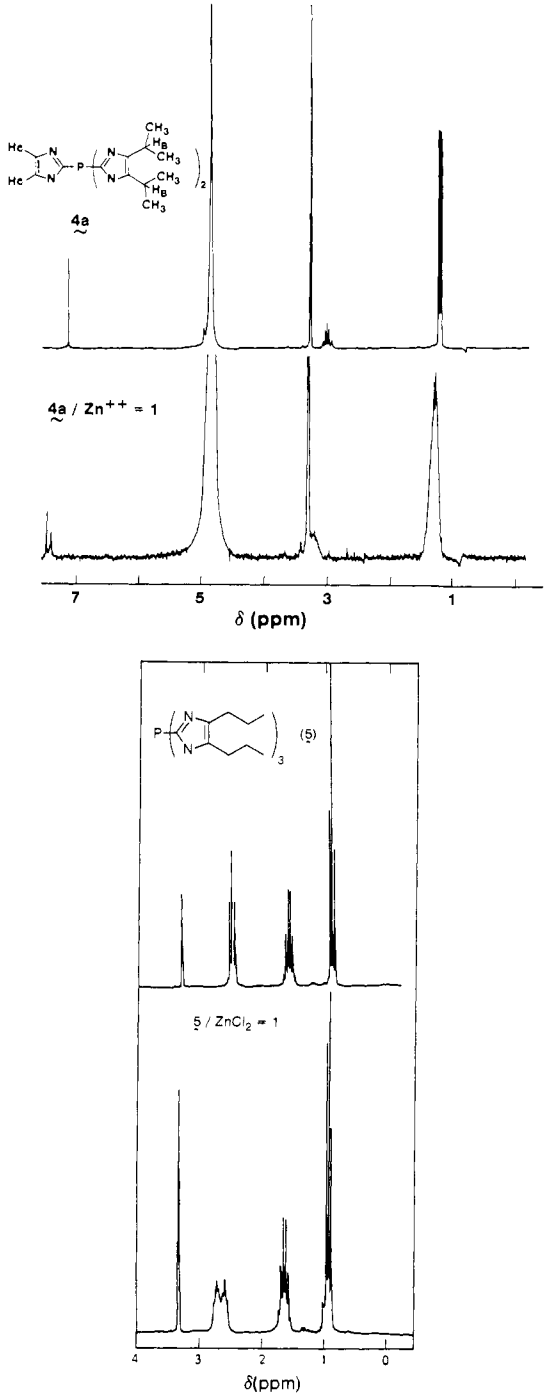

Figure 1. (a, top) ^{1}H NMR spectrum of **4a** as a function of added $ZnCl_2$. Resonances centered at δ 4.8 and 3.3 are from HOD and deuteriomethanol solvents. (b, bottom) ^{1}H NMR spectrum of **5** as a function of added $ZnCl_2$.

is the initial concentration of HCO_3^-, which for these experiments varies from 1×10^{-4} to 2.5×10^{-3} M. The values determined in this way have a precision of 5% or better.

The effects of inhibitory anions were determined at a pH which corresponds to the maximum values for k_{cat}^{obsd}, 6.55 for ligands **4a,b** and 6.45 for ligand **5**. Anions were introduced into the syringe containing buffer, indicator, and ligand and values of k_{obsd} and k_f determined as above.

Results

A. Synthetic pathways for the construction of ligands **1c**, **4a**, **4b**, and **5** are shown in Scheme I. For the most part, the syntheses are routine with the exception of that of *N*-(dimethoxymethyl)-4,5-diisopropylimidazole,[13] which differs slightly from

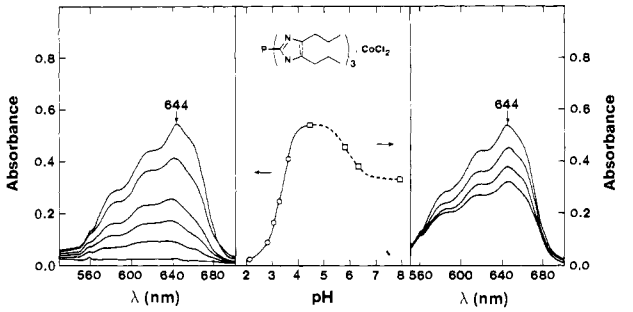

Figure 2. Visible absorption spectra of **5**·$CoCl_2$ (7.5×10^{-4} M, 0.2 M NaCl) as a function of pH. Left-hand spectra increase in intensity from pH 2 to 4.5; right-hand spectra decrease in intensity from pH 4.5 to 8. Solvent 80% EtOH–H_2O.

the procedure we reported in ref 5.

B. Ligand pK_a and pK_M^{2+} values are listed in Table I. Like all ligands we have studied that accelerate the $HCO_3^- \rightleftarrows CO_2$ interconversion, **4a**, **4b**, and **5** have a greater propensity to bind with Zn^{2+} than Co^{2+}, as does CA,[14] which may result from an enforced low-coordinate geometry.

Quantitative titration experiments on solutions consisting of equimolar $Zn^{2+}(ClO_4^-)_2$ and ligand with 2 equiv of added H^+ show that all H^+ is accounted for by pH 6 (**4a**·Zn^{2+}) and 5.8 (**5**·Zn^{2+}). That these values are substantially lower than in the absence of Zn^{2+} (all H^+ is consumed only after pK_{a_3} of the ligand has been passed) indicates that a complex is fully formed by these pHs, with the Zn^{2+} being coordinated in a tridentate fashion, or bidentate with the nonassociated imidazole remaining nonprotonated. More than likely (vide infra) these two (and possibly other) states are in rapid equilibrium. Although it appears in continuing the titration that some additional ionization of H^+ is commencing, no well-defined pK_a is obtained since precipitation occurs above pH 7 at the concentrations required for titration.

^{1}H NMR analysis of the nature of L·Zn^{2+} binding was undertaken on 0.02 M solutions of **4a** or **5** in methanol-d_4 as a function of added aliquots of $ZnCl_2/D_2O$. As is shown in Figure 1a, when the **4a**/Zn^{2+} ratio is 1, the original signals attributable to **4a** have been replaced with broadened isopropyl resonances centered at δ 1.3 (CH_3's) and 3.2 (C–H) while the imidazole 4 and 5 H's appear as separate signals at δ 7.4 and 7.5 downfield due to their proximity to Zn^{2+}. Further addition of Zn^{2+} produces no additional changes in the spectrum, and hence the lower trace in Figure 1a is that of a 1:1 complex experiencing a dynamic exchange process involving the isopropylimidazoles and Zn^{2+}.

The situation for **5** is quite different as is shown in Figure 1b. Here, when the **5**/Zn^{2+} ratio is 1, the CH_2 groups at the 4 and 5 positions are clearly split into two overlapping triplets centered at δ 2.6 and 2.75, as is expected if tridentate complexation occurs and dynamic exchange on the NMR time scale is slow. Further additions of $ZnCl_2$ do not alter the spectrum. It is of note that if the same experiment is conducted using aliquots of $Zn(ClO_4)_2$ the situation is somewhat different in that the finally produced spectrum does not show evidence of two chemical shift inequivalent resonances for the imidazole 4 and 5 methylene units but rather a single broadened signal centered at δ 2.68. Such would indicate that the nature of the L·Zn^{2+} complex and its dynamic exchange properties is dependent upon the presence of added anions.

C. Co(II) Absorption Spectra. As is well-known, the Zn^{2+} of native CA can be replaced with Co(II) leading to a reddish blue

(13) Our original procedure[5] for protecting 4,5-diisopropylimidazole[7] as is *N*-(dimethoxymethyl)acetal involved refluxing a toluene suspension trimethyl orthoformate and the imidazole in the presence of toluenesulfonic acid and removing $HOCH_3$ as it is formed. We were unable to reproduce this synthesis in satisfactory yield with fresh samples of trimethyl orthoformate. Further investigation indicated that the original reagent had been contaminated with HCO_2H by hydrolysis, and it was this acid which proved to be essential. Yields in excess of 75–80% can routinely be obtained on ~0.1 M scale if 2 mL of HCO_2H is added to the reaction mixture.

(14) (a) Lindskog, S. *J. Biol. Chem.* **1963**, *238*, 945–951; $pK_{Zn}^{2+} = 10.5$, $pK_{Co}^{2+} = 7.2$. (b) Lindskog, S.; Nyman, P. O. *Biochim. Biophys. Acta* **1964**, *85*, 462–474.

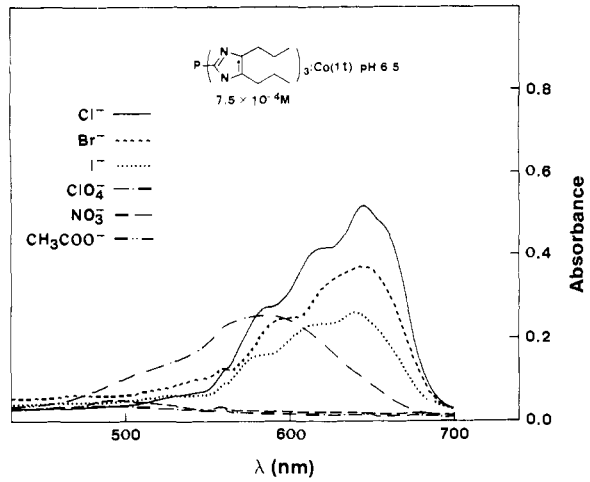

Figure 3. Visible absorption spectra of **5**·Co(II) (7.5×10^{-4} M, 80% EtOH–H_2O) in the presence of various anions.

Table II. k_{obsd} Values for $HCO_3^- + H^+ \rightarrow$ Dehydration[a,b]

pH[c]	[0]	k_{obsd} (s^{-1})[c,d] 4a·Zn^{2+}	5·Zn^{2+}	k_{cat}^{obsd} M^{-1} s^{-1} [e] 4a·Zn^{2+}	5·Zn^{2+}
6.20	1.13	1.13	1.68	0	2200
6.30	0.97	1.10	1.53	520	2240
6.45	0.80	1.08	1.45	920	2400
6.55	0.65	1.03	1.27	1520	2480
6.70	0.455	0.75	1.02	1200	2260
6.80	0.42	0.58	0.86	640	1760

[a] 80% EtOH/H_2O (v/v), 25.0 ± 0.2 °C, 1×10^{-3} M $NaHCO_3$, 2.5×10^{-2} M HEPES, ionic strength 0.2 M ($NaClO_4$), catalyst = 2.5×10^{-4} M when present. [b] Followed by monitoring the appearance of bromocresol purple anion at 600 ± 20 nm, [BCP] = 5×10^{-4} M. [c] Comparison values made at a given pH by reading values from Figure 4. pH refers to starting value, with changes <0.05 unit except for pH 6.2 which changed by ~0.1 unit. [d] Values of k_{obsd} ±0.03 unit. [e] Defined as in eq 5.

enzyme with ~45% the catalytic activity of the natural form.[14a,15a] The absorption spectrum is characteristic of a 4- and/or 5-coordinate metal ligation[15b] which is sensitive to the pH of the solutions. Depending upon the conditions of measurement, the spectroscopic pK_a of Co(II)CA can vary from ~5.6 to values in excess of 7 in the presence of added monovalent anions,[15c-e] the latter also perturbing the Co(II) absorption spectrum in a characteristic way by associating with the metal.

For equimolar **4a** and $CoCl_2$ the absorption spectrum as a function of pH shows only little formation of a 4-coordinate complex since ϵ_{max} in the 600-nm region is ~15 M^{-1} cm^{-1} rather than the expected[15b] 10^2–10^3 M^{-1} cm^{-1}. However, the situation for **5**·Co(II) is quite different, and as shown in Figure 2, solutions of 7.5×10^{-4} M in each of **5** and $CoCl_2$ with 0.2 M of added NaCl show buildup of a tetrahedral complex between pH 2 and 4.5 (ϵ_{max}^{644} = 720 M^{-1} cm^{-1} at pH 4.5 assuming complete 1:1 binding). Above pH 4.5, the intensity of the band at 644 nm diminishes, as does its overall appearance which indicates gradual formation of a second 4- or 5-coordinate complex (ϵ_{max}^{644} = 427 at pH 8 assuming 1:1 binding). By measuring quantitatively the consumption of OH^-, it is apparent that OH^- is consumed during the course of the transformation by association with the Co(II) or by titration of a metal-bound H_2O. From Figure 2, the apparent pK_a for this process is roughly 6. No indication of blue colored complexes is seen if ClO_4^- or NO_3^- ions are used as counterions, which indicates that the pH-dependent low-coordinate complexes must have associated Cl^- in at least one of the ligand positions.

(15) (a) Lindskog, S.; Malmström, B. G. *J. Biol. Chem.* **1962**, *237*, 1129–1137. (b) Bertini, I.; Canti, G.; Luchinat, C.; Scozzafava, A. *J. Am. Chem. Soc.* **1978**, *100*, 4873–4877. (c) Bertini, I.; Luchinat, C.; Scozzafava, A. *Inorg. Chim. Acta* **1980**, *46*, 85–89. (d) Jacob, G. S.; Brown, R. D.; Koenig, S. *Biochemistry* **1980**, *19*, 3755–3765. (e) Koenig, S. H.; Brown, R. D.; Jacob, G. S. In "Biophysics and Physiology of Carbon Dioxide"; Bauer, C., Gros, G., Bartels, H., Eds.; Springer-Verlag: Berlin, 1980; pp 238–253.

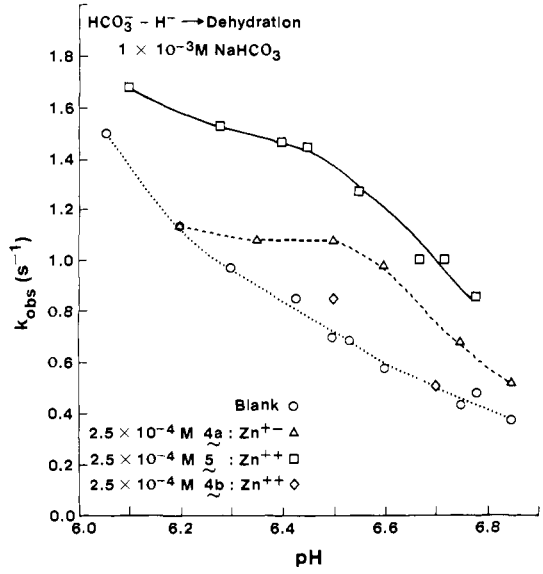

Figure 4. k_{obsd} as a function of pH for $HCO_3^- \rightleftarrows CO_2$ equilibration approached from HCO_3^- dehydration: (○) no catalyst, (△) 2.5×10^{-4} M **4a**·Zn^{2+}, (□) 2.5×10^{-4} M **5**·Zn^{2+}, (◇) 2.5×10^{-4} M **4b**·Zn^{2+}, 80% EtOH–H_2O, 0.2 M $NaClO_4$, 5×10^{-4} M bromocresol purple indicator, 1×10^{-3} M $NaHCO_3$, 2.5×10^{-2} M HEPES.

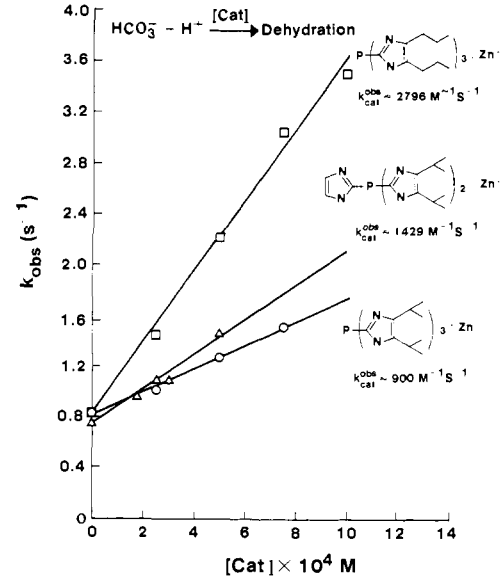

Figure 5. k_{obsd} for $HCO_3^- \rightleftarrows CO_2$ equilibration as a function of [catalyst]: 80% EtOH–H_2O, 0.2 M $NaClO_4$, 5×10^{-4} M bromocresol purple indicator, 1×10^{-3} M $NaHCO_3$, 2.5×10^{-2} M HEPES; (□) **5**·Zn^{2+}, initial pH 6.45; (○) **1c**·Zn^{2+}, pH 6.45; (△) **4a**·Zn^{2+}, pH 6.55.

As is shown in Figure 3, the Co(II) absorption spectrum is indeed anion dependent, with Cl^-, Br^-, and I^- giving evidence of tetrahedral complexes, while $CH_3CO_2^-$ and HCO_2^- (the latter not shown in Figure 3) are probably 5-coordinate.[15b]

D. Kinetic Studies. (a) k_{obsd} Measured from the Direction of $HCO_3^- + H^+ \rightarrow$ Dehydration. Plots of k_{obsd}, as defined in eq 3 and 4 against pH are shown in Figure 4, the data being given in Table II. It can be seen that the largest difference between the blank and catalyzed reactions occurs with **5**·Zn^{2+} followed by **4a**·Zn^{2+}, the difference being maximal at pH 6.4–6.5. (The **4b**·Zn^{2+} complex shows only small activity at pH 6.5 and no detectable catalytic effect at any other pH values so that further study was discontinued.)[16] As in the case of our previously

(16) We note here however that the overall structure of **4b**·Zn^{2+} could be taken as a reasonable model for the active site of alkaline phosphatase. Phosphatase and esterase activities of this and related complexes are presently under investigation in these laboratories and will be reported in due course. Brown, R. S.; Zamkani, M. unpublished results.

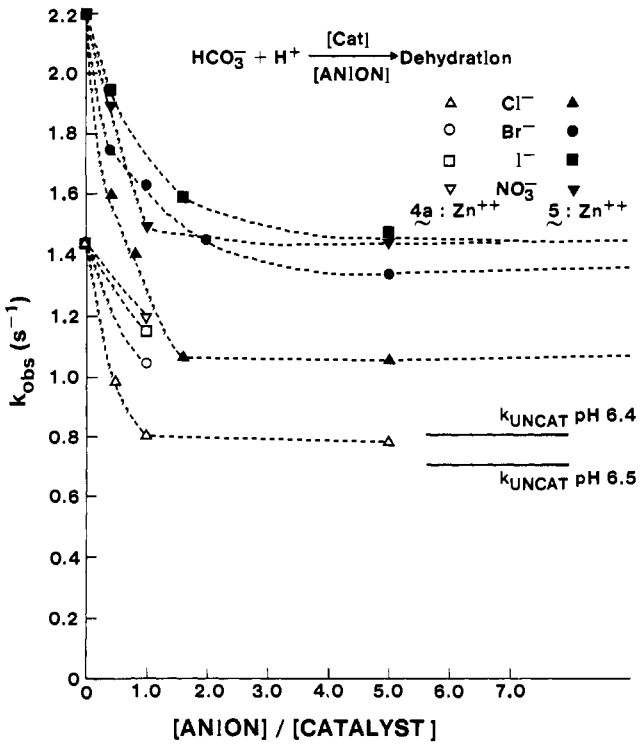

Figure 6. Effect of added inhibitory anions on k_{obsd} determined in the presence of 5×10^{-4} M **5**·Zn^{2+} (closed symbols, pH 6.45) and 5×10^{-4} M **4a**·Zn^{2+} (open symbols, pH 6.55). 80% EtOH–H_2O, 0.2 M $NaClO_4$, 5×10^{-4} M bromocresol purple indicator, 1×10^{-3} M $NaHCO_3$, 2.5×10^{-2} M HEPES.

reported catalyst, **1c**·Zn^{2+}, the activities of the above are nearly completely lost at pH <6 and >7, for reasons which seem attributable to protonation of the ligand at low pH and OH^- sequestering of the Zn^{2+} from the complex at high pH, both processes leading to inactive species.[3a]

Shown in Figure 5 is the relationship between k_{obsd} and [catalyst] for each of **1c**·Zn^{2+},[3a] **4a**·Zn^{2+}, and **5**·Zn^{2+} at the pHs which correspond to their maximal activities (6.4, 6.5, and 6.4, respectively). For this relationship the initial [HCO_3^-] was 1×10^{-3} M, although as will be shown later, there is a dependence of k_{obsd} upon this. Control experiments using ligand or Zn^{2+} alone established that no catalysis is apparent since k_{obsd} measured was the same as that seen for the blank reaction. Hence catalytic viability requires a cooperative interaction between ligand and Zn^{2+} as was reported earlier for **1c**·Zn^{2+}.[3a] A final control established that k_{obsd} is independent of [BCP].

(b) Effect of Added Monovalent Anions on k_{obsd}. It has long been recognized that monovalent anions inhibit the activity of CA,[1,14a,11,17] noncompetitively, or uncompetitively[18] for CO_2 hydration and competitively for HCO_3^- dehydration. In order to test whether monovalent anions also diminish the activity of these catalysts, studies were undertaken at the optimal pH for each, the data for **4a**·Zn^{2+} and **5**·Zn^{2+} being given in Table III. It can be seen from Figure 6 that these anions prove to be inhibitors, as is the case with **1c**·Zn^{2+}.[3a] However, k_{obsd} eventually levels off with increasing [anion] to a value which is still greater than that for the uncatalyzed process. This would indicate that a ternary complex is formed between catalyst and anion and furthermore that this complex is still catalytically viable. No effect of added anion is seen on k_{obsd} for the uncatalyzed blank reactions.

(c) Effect of [$NaHCO_3$] on k_{obsd}. Since the above experiments indicate an association of anions and catalyst, a study was un-

Table III. Effects of Added Monovalent Anions on k_{obsd}[a]

[anion]/[catalyst]	NaCl	NaBr	NaI	$NaNO_3$
k_{obsd} (s^{-1}) [4a·Zn^{2+}] 5×10^{-4} M, pH 6.50[b,c]				
0.0	1.43	1.43	1.43	1.43
0.5	0.98			
1.0	0.79	1.04	1.15	1.19
5.0	0.78			
k_{obsd} (s^{-1}) [**5**·Zn^{2+}] 5×10^{-4} M, pH 6.45[b,d]				
0.0	2.21	2.21	2.21	2.21
0.4	1.60	1.74	1.94	1.89
0.8	1.40			
1.0		1.63		1.48
1.6	1.06		1.59	
2.0		1.45		
5.0	1.08	1.33	1.47	1.49

[a] Temperature = 25.0 ± 0.2 °C, [$NaHCO_3$] = 1×10^{-3} M, [indicator] = 5×10^{-4} M, 80% EtOH–H_2O (v/v), [HEPES] = 2.5×10^{-2} M, total ionic strength including added anion = 0.2 M ($NaClO_4$). [b] Values ±0.03 s^{-1}. [c] Uncatalyzed k_{obsd} invariant with [anion], 0.70 s^{-1}. [d] Uncatalyzed k_{obsd} invariant with [anion], 0.80 s^{-1}.

Table IV. Effect of [$NaHCO_3$] on k_{obsd}[a]

	k_{obsd} (s^{-1})					
	1c·Zn^{2+}[b] (5×10^{-4} M)		4a·Zn^{2+}[b] (5×10^{-4} M)		**5**·Zn^{2+}[c] (2.5×10^{-4} M)	
[$NaHCO_3$] ($\times 10^4$ M)	no Cl^-	5×10^{-4} M Cl^-	no Cl^-	5×10^{-4} M Cl^-	no Cl^-	5×10^{-4} M Cl^-
3.0	0.95	0.63	1.0		1.29	0.90
5.0		0.65	1.07		1.53	1.03
7.5	1.05		1.27		1.55	
10.0	1.10	0.69	1.42	0.72	1.58	1.15
17.5	1.16		1.59		1.71	1.25

[a] Temperature = 25.0 ± 0.2 °C, 80% EtOH/H_2O (v/v), 5×10^{-4} M bromocresol purple, ionic strength = 0.2 M ($NaClO_4$). [b] pH 6.55; k_{obsd} in the absence of catalyst = 0.63 s^{-1} and is invariant with [$NaHCO_3$] and added Cl^-. [c] pH 6.45; k_{obsd} in the absence of catalyst = 0.80 s^{-1} and is invariant with [$NaHCO_3$] and added Cl^-.

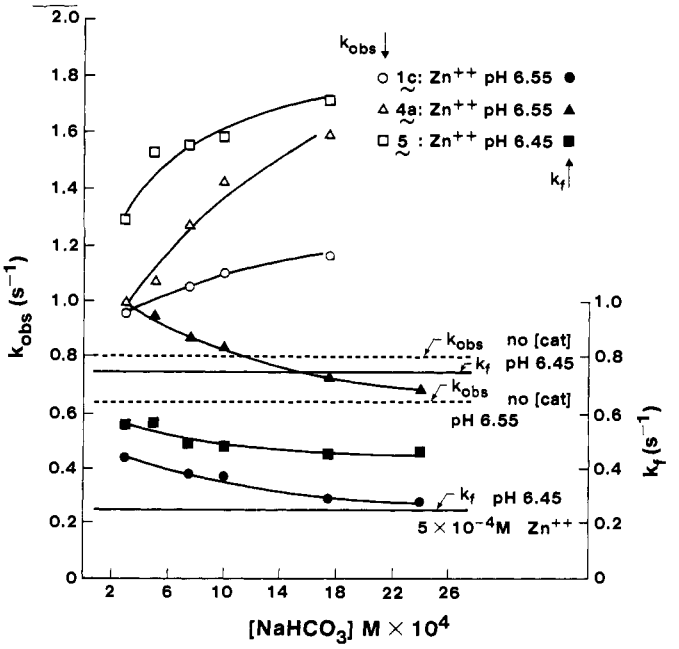

Figure 7. k_{obsd} (open symbols) and apparent k_f (closed symbols) as a function of initial [$NaHCO_3$]. Dashed horizontal lines represent k_{obsd} determined with no added catalyst at pH 6.45 and 6.55 while the two continuous horizontal lines represent apparent k_f in the presence of 5×10^{-4} M Zn^{2+} alone, pH 6.45. 80% EtOH–H_2O, 0.2 M $NaClO_4$, 5×10^{-4} M bromocresol purple, 2.5×10^{-2} M HEPES.

(17) (a) Roughton, F. J. W.; Booth, V. H. *Biochem. J.* **1946**, *40*, 319–330. (b) Meldrum, N. U.; Roughton, F. J. W. *J. Physiol. (London)* **1933**, *80*, 143–170. (c) King, R. W.; Burgen, A. S. V. *Proc. R. Soc. London, Ser. B* **1976**, *193*, 107–125.
(18) (a) Pocker, Y.; Diets, T. L. *J. Am. Chem. Soc.* **1982**, *104*, 2424–2434. (b) Pocker, Y.; Diets, T. L. *Ibid.* **1983**, *105*, 980–986.

dertaken to determine whether changes in [$NaHCO_3$] affected k_{obsd} in a way which might be indicative of a saturation phenomenon. The data obtained for **1c**·Zn^{2+}, **4a**·Zn^{2+}, and **5**·Zn^{2+} at their optimal pHs are given in Table IV and displayed in Figure 7 as the open symbols. Ideally it would be preferable to perform these experiments over as wide a range of [$NaHCO_3$] as possible; however, values less than 2.5×10^{-4} M produced extremely small changes in absorbance, while those greater than 17.5×10^{-4} M led to pH changes in excess of 0.1 unit and therefore were inappropriate to give meaningful results for k_{obsd}. However, since in the absence of catalyst, changes in [$NaHCO_3$] do not change k_{obsd} (shown in Figure 7 as the dashed horizontal lines), the observation that k_{obsd} in the presence of catalyst increases with increments in [$NaHCO_3$] in a less than first-order way indicates a saturation phenomenon of some sort in which HCO_3^- binds to the catalyst in an equilibrium prior to the dehydration step.

(d) Initial Rate Measurements. Initial rate experiments were conducted as described in the Experimental Section from the direction of $HCO_3^- + H^+ \rightarrow$ dehydration by evaluating the slopes of absorbance vs. time plots for the first 5% of the reaction. Separate determinations were made in the absence and presence of added catalyst as well as in the presence of 5×10^{-4} added Zn^{2+} alone. The results are presented graphically in Figure 7 as the closed symbols. The most curious trend is the gradual diminution in apparent k_f with increasing [$NaHCO_3$] when catalyst is present which we believe is due to an experimental artifact.[11h]

Discussion

(a) Mode of M^{2+} Binding by 4 and 5. Although the metal-binding constants given in Table I indicate that ligands **4** and **5** have large affinities for Zn^{2+} and Co^{2+}, it would appear from the NMR studies that the nature of the complexes depends upon counterions which are also associated with the M^{2+}. Since the quantitative titration experiments performed on solutions containing equimolar ligand and Zn^{2+} as well as added H^+ indicate that all added protons are accounted for by pH 6 (for **4a**) and 5.8 (for **5**), it is safe to conclude that the complexes are fully formed by that point, with none of the associated imidazoles being protonated. This finding alone does not show that the ligands are bound in a tridentate fashion. However, such is clearly implied, at least for **5**·$ZnCl_2$ by the appearance of the ^1H NMR spectrum of the complex shown in Figure 1b. Since the resonances of the CH_2 groups on the 4 and 5 positions of the imidazoles in the 1:1 $ZnCl_2$ complex are of equal intensity but chemical shift inequivalent, they must reside on the average at different distances from the bound Zn^{2+}, as is expected for a rigid tridentate complex. This excludes other modes of binding such as through two imidazoles and/or P since the appearance of the spectrum would necessarily be different. Moreover, such a rigid tridentate complex is clearly dependent on the presence of Cl^-, since when $Zn(ClO_4)_2$ is used the NMR spectrum of the 1:1 complex is indicative of a dynamic exchange process which brings the 4 and 5 CH_2 resonances into a more averaged environment, probably by imidazole debinding, tautomerization, and rebinding as in **7** and **7a** (Y = associated anion or solvent).

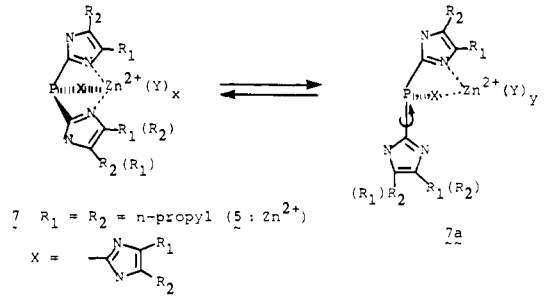

7 $R_1 = R_2$ = n-propyl (**5** : Zn^{2+})

X =

7a

For **4a**·Zn^{2+} the ^1H NMR spectra are similar in the presence of either Cl^- or ClO_4^- and show broadened isopropyl resonances so the exchange in these complexes is fast. Curiously, the 4 and 5 H's of the simple imidazole appear as discrete signals of slightly different shape (since their coupling possibilities with adjacent nuclei differ), which likely indicates that its exchange rate is slower than that of the diisopropylimidazoles.

Similarly, the Co(II) visible absorption spectra of **5**·Co(II) complexes show a strong dependence on the presence or associated anions (Figure 3). Such complexes are forced by the presence of ligand to be 4-coordinate in the cases of halide but with acetate and formate appear to be 5-coordinated.[15b] Since in the presence of ClO_4^- and NO_3^- alone there is no evidence for a "blue" 4- or 5-coordinate species, it is clear that low-coordinate **5**·Co(II) complexes require an associated anion at at least one of the available metal sites. This is also observed in the case of **1c**·Co(II)[3a] but not **2**·Co(II).[3c] Apparently **4a**·Co(II) shows some minor tendency to adopt a low-coordinate complex as evidenced by a faint blue color, but on the basis of the anticipated absorbance in the 600-nm region, most of the complexes in solution must be octahedral.

Finally, we consider the absorbance vs. pH profile for **5**·$CoCl_2$ shown in Figure 2. On the basis of the consumption of OH^- during the course of this process it can be concluded that by pH 4.5, the tetrahedral complex is free from protonation and likely consists of tridentate chelation of Co(II) by **5** and a single associated Cl^- as in **8** (eq 8). Further increases in pH cause a change in the

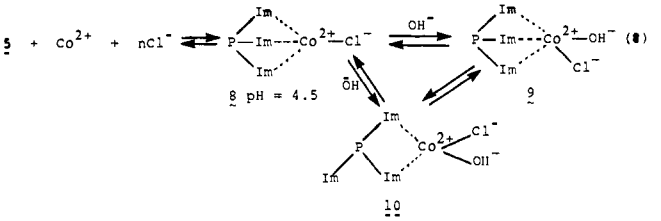

8 pH = 4.5 **9**

10

nature of the blue species in solution, and since additional OH^- is consumed the complex(es) present at pH 8 must have an associated OH^- as in **9** or **10**. Although there is precipitation above pH 8, one can set a lower limit for the apparent "pK_a" pertaining to this process at ~6 or slightly higher (cf. Figure 2). However, since no blue color is seen if only ClO_4^- is present, both **9** and **10** must have an associated Cl^-.

(b) Kinetic Studies of k_{obsd}. In an 80% EtOH/H_2O medium, the attainment of the equilibrium of $HCO_3^- \rightleftarrows CO_2$ interconversion is a relatively rapid process having an uncatalyzed half time of some 0.5 to 1.7 s between pH 6.05 and 6.85, respectively. As was the case in our previously reported studies,[3a,c] under the appropriate buffering conditions the process in eq 3 can be considered in terms of a simple first-order equilibrium in which k_{obsd} is equivalent to the sum of all pseudo-first-order rate constants in the dehydration and hydration directions and hence can be thought of as a measure of the rapidity with which equilibrium is attained. From Figure 4 it can be seen that added complex speeds the reaction but only over a fairly narrow range between pH 6–7.

Maximal activities for each of **1a**·Zn^{2+}, **4a**·Zn^{2+}, and **4b**·Zn^{2+}, and **5**·Zn^{2+} are exhibited at 6.4–6.5. Disappointingly, the activity of **4b**·Zn^{2+} (represented by ◊ on Figure 4) is smaller than that of **4a**·Zn^{2+} even though the former contains a hydroxyethyl group as a mimic for the threonine OH group associated with the enzyme's active site which has been suggested to be of importance in the catalytic cycle.[2a] Our original expectation was that if any of the possible **4b**·Zn^{2+} complexes resembled that in **11**,[19] the

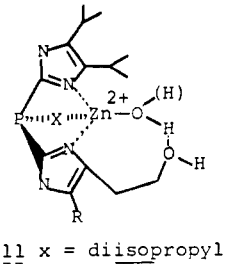

11 x = diisopropylimidazole

R = H

association of the hydroxyethyl group and a Zn^{2+}–OH_2 might resemble that proposed for the enzyme[2a] and lead to a decidedly larger activity than seen for **4a**·Zn^{2+}. The observation of minimal activity would either indicate such association is not important or more likely (given the imperfect nature of any model) that the geometry of metal binding is such that the hydroxyethyl group is on the average not restricted to be in the vicinity of the metal.[16,19a,b] The following discussions will therefore be limited to **4a**·Zn^{2+} and **5**·Zn^{2+}.

From Figure 5 it can be seen that a linear relationship exists between [catalyst] and k_{obsd}. Comparatively, from the slopes of the lines, the relative catalytic ratios of **5**·Zn^{2+}, **4a**·Zn^{2+}, and previously reported **1c**·Zn^{2+} [3a] is 3:1.7:1. Without knowledge of the nature of the active species, it is difficult to ascertain what features for a given case are important for rate enhancement. However, as was previously stated, X-ray crystallographic analysis of **1c**·$Zn^{2+}Cl_2^-$ [3b] indicated that the three diisopropylimidazoles encapsulate the Zn^{2+} ion in such a restrictive way (**12a**) that exchange of reactants at the remaining metal site would require a 5-coordinate complex (**13a**) which is undoubtedly severely buttressed (eq 9). Since at least one[2a] of the several postulated

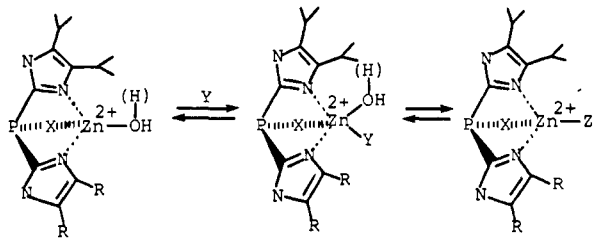

12 a; R = isopropyl 13 a; R = isopropyl 14
b; R = H b; R = H

(9)

mechanisms for CA[1] involves an association of both (H)OH and CO_2 in a 5-coordinate complex during the catalytic cycle, it appeared likely that the **4a**·Zn^{2+} complex would have greater accessibility of the reagents to the metal surface as in **12b** → **13b** and at the same time retain low coordination numbers around the metal. Since **4a**·Zn^{2+} is indeed more active than **1c**·Zn^{2+}, this expectation appears to be borne out, although the magnitude of the enhancement falls far short of what would be considered definitive.

The **5**·Zn^{2+} complex is more active yet likely results from a combination of factors relating to increased accessibility of reagents to the Zn^{2+} which resides in a more hydrophobic environment. X-ray analysis of CA[2] indicates that the essential Zn^{2+} sits at the bottom of a cavity some 10 Å deep lined on one side with hydrophobic residues and the other with hydrophilic residues. From molecular models of a tricoordinated **5**·Zn^{2+}, it can be deduced that the *n*-propyl groups are not only more flexible than the isopropyl groups of **1c**·Zn^{2+} which should lead to easier reactant accessibility to the metal surface, but since the *n*-propyl groups can extend outward into the solution they provide a deeper hydrophobic pocket in which the catalytic event can occur. Since earlier studies[20] indicated that the simple trisimidazolylphosphine complexes **1a**·Zn^{2+} and **1b**·Zn^{2+} are inactive, while **1c**·Zn^{2+} and **5**·Zn^{2+} are increasingly active, it would appear that providing a hydrophobic environment for the bound Zn^{2+} is an important consideration for these models.[21]

Further experiments with **4a**·Zn^{2+} also indicate that the composition of medium has important consequences on catalysis. For reasons of solubility, the medium chosen for **1c**·Zn^{2+} and **5**·Zn^{2+} requires at least 80% EtOH. However, **4a**·Zn^{2+} is somewhat more soluble in solutions containing increased amounts of water. It was observed that as the solvent composition changed from 60 → 70 → 80 → 90% ethanol, k_{obsd} for the blank uncatalyzed reaction was invariant at 0.63 s^{-1} (pH 6.5),[22] but the reactions in media containing 2.5×10^{-4} M **4a**·Zn^{2+} exhibited k_{obsd} values of 0.68, 0.89, 1.09, and 1.12 s^{-1}, respectively (±0.03 s^{-1}). Hence activity is greatest in media having ≳80% ethanol content, again supporting the idea that a hydrophobic environment is important for optimal activities.

(c) Effects of Added Inhibitory Anions on k_{obsd}. Enzymatically, the presence of monovalent anions has been shown to inhibit the activity of CA,[1,14a,11,17] and the bulk of the evidence indicates that these inhibitors exert their effect by association with the active site Zn^{2+}, thereby preventing access of the reagents (H_2O and CO_2 or HCO_3^-). Recent elegant work from Pocker's laboratories[18] indicates that like other anions, HCO_3^- is an inhibitor of CO_2 hydration, and furthermore that at high pH, an observed "linear uncompetitive" mechanism of inhibition requires that the inhibitor binds to a fifth metal coordination site after CO_2 is in place.

From the data of Table III which are displayed in Figure 6, added monovalent anions also diminish the activity of catalysts **4a**·Zn^{2+} and **5**·Zn^{2+} as they do **1c**·Zn^{2+}. The fact that Cl^- substantially reduces k_{obsd} for both at $[Cl^-]$/[catalyst] ratios of <1 but has little additional effect at ratios >1 such that there is still some residual catalytic activity indicates not only that there is a large formation constant for a ternary catalyst–anion complex but that this complex is capable of associating with HCO_3^- in a catalytically competent way. The simplest scheme is shown in eq 10 where L represents **4a** or **5**. The fact that increasing

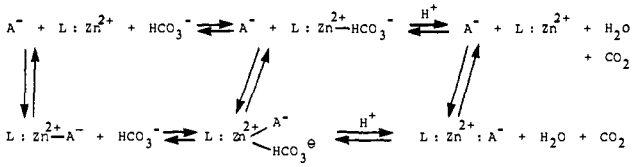

(10)

$[HCO_3^-]$ leads to larger values of k_{obsd} for **5**·Zn^{2+} even in the presence of 5×10^{-4} M Cl^- (Table IV) indicates either a competition in which the inhibitory anion can be displaced from the Zn^{2+} by increasing $[HCO_3^-]$ or that a new also active ligand-coordinated A^-–Zn^{2+}–HCO_3^- quaternary complex is produced, neither eventuality being distinguished by the available data.

Since each of the above experiments seemingly indicates an equilibrium association of anions (including HCO_3^-) and *L*·Zn^{2+} prior to a catalytic step, we sought to provide evidence for a saturation effect on k_{obsd} by increasing [$NaHCO_3$]. Experiments relating k_{obsd} and [$NaHCO_3$] at pH 6.45 and 6.55 were conducted in the absence and presence of 5×10^{-4} M added [cat], the data being given in Table IV and k_{obsd} being illustrated in Figure 7 as the open symbols. In the absence of any catalyst, k_{obsd} does not change as a function of $[HCO_3^-]$, verifying the pseudo-first-order nature of this process. However, in the presence of

(19) (a) We recognize that if the **4b**·Zn^{2+} complex is in a dynamic equilibrium mixture of complexes differing in coordination number or mode of binding, then it may be that the hydroxyethyl group could have been on the distal side of a bound imidazole (represented by R in **11**) or that the (hydroxyethyl)imidazole itself was not bound. ^1H NMR experiments on the mode of Zn^{2+} binding by **4b** showed that the imidazole 4(5) H shifts to lower field in the presence of Zn^{2+}, as expected if the imidazole is associated, but broadens considerably indicating some dynamic process. However, since the activity exhibited by **4b**·Zn^{2+} is much lower than for **4a**·Zn^{2+}, it cannot be contended that any of the configurations of **4b**·Zn^{2+} are tremendously active. (b) NMR evidence of **4b**·$ZnCl_2$ in MeOH-d_4 indicates that there are two dominant complexes formed (~1:1 ratio) which differ by having the hydroxyethyl group of the simple imidazole at the proximal and distal site respectively relative to the bound Zn^{2+}. In addition, the remaining two diisopropylimidazoles are undergoing a sufficiently rapid site exchange that they appear as a broadened signal akin to that described herein for **4a**·Zn^{2+} (Figure 1a). Hence a structure not unlike **11** is possible.

(20) Huguet, J.; Brown, R. S. *J. Am. Chem. Soc.* **1980**, *102*, 7571–7572.

(21) Originally Tabushi[4d] studied a bidentate model consisting of a cyclodextrin containing two pendant imidazoles that suggested that hydrophobicity was an integral factor in designing catalysts for $CO_2 \rightleftarrows HCO_3^-$ interconversion.

(22) Although "pH" for these reactions are simply those read from an electrode immersed directly in the buffered solution, we recognize that the activity of H^+ is changing (Bates, R. G.; Paabo, M.; Robinson, R. A. *J. Phys. Chem.* **1963**, *67*, 1833–1838). Nevertheless, comparison between the uncatalyzed and catalyzed k_{obsd} in the changing medium does indicate that the catalyst is increasingly active as ethanol content increases.

catalysts **1c**, **4a**, and **5**·Zn^{2+} the situation is markedly different and indicative of a saturation phenomenon. Unfortunately, for reasons pertaining to experimental limitations discussed previously, we were unable to study $[HCO_3^-]$ outside the region of (2.5–17.5) $\times 10^{-4}$ M. Nevertheless, so far as we are aware, the observations represent the first finding of a saturation phenomenon for a model catalyzing $HCO_3^- \rightleftarrows CO_2$ equilibration. The simplest scheme accommodating these data is given in eq 11 although on the basis

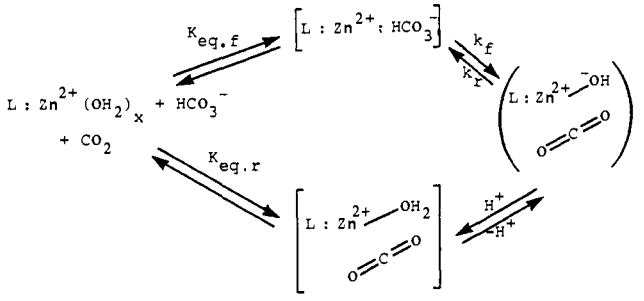

(11)

of the above experiments we cannot evaluate the individual constants[23] or ascertain the existence of a $L{\cdot}Zn^{2+}CO_2$ complex.

(d) Initial Rate Experiments. In an effort to provide values for the association constant of $L{\cdot}Zn^{2+}$ and HCO_3^-, and k_{fmax} (the maximal forward rate constant for the $L{\cdot}Zn^{2+}{\cdot}HCO_3^-$ complex), initial rate experiments were performed from the direction of

$$HCO_3^- + H^+ \xrightarrow{k_f} \text{dehydration}$$

and k_f evaluated at initial $[HCO_3^-]$ from (3–25) $\times 10^{-4}$ M, the results being graphically presented in Figure 7 as the closed symbols. Firstly, in the absence of added ligand or Zn^{2+}, it is observed that the apparent k_f is invariant with increasing $[HCO_3^-]$. From a knowledge of $k_{obsd} = (k_f + k_r)$ the equilibrium constant at pH 6.45 could be determined as $K_{eq\ 6.45} = k_f/(k_{obsd} - k_f) \simeq 0.72\ s^{-1}/0.08\ s^{-1} \simeq 9$. Hence from the direction of HCO_3^- dehydration, apparently the reaction proceeds almost entirely to CO_2 in this medium at pH 6.45.

Unexpectedly, the results obtained in the presence of added Zn^{2+} shows that k_f apparently is reduced even though k_{obsd} remains unchanged from that seen in the absence of Zn^{2+} (Figure 7). If taken literally, this requires that k_r must increase to maintain the value of k_{obsd} and hence leads to the unlikely scenario that the $HCO_3^- \rightleftarrows CO_2$ equilibrium constant must dramatically shift in the presence of Zn^{2+} but in some fashion independent of the $[Zn^{2+}]/[HCO_3^-]$ ratio. Moreover, in the presence of ligand·Zn^{2+} the observation appears to be that k_f actually diminishes with increasing $[NaHCO_3]$ even though k_{obsd} is increasing. If taken literally, this leads to the improbable conclusion that K_{eq} observed in the presence of catalyst not only varies as a function of increasing $[HCO_3^-]$, but in the high concentration limit lies more to the side of bicarbonate even though the bulk of HCO_3^- present in solution is not associated with complex and should proceed to CO_2 at the same rate as when catalyst is not present. Clearly each of the above impossibilities indicates that in this situation the apparent k_f is not a true measure of the HCO_3^- dehydration. In order to convince ourselves that this was indeed an experimental artifact, visible absorption spectra of buffered solutions containing BCP, $Zn(ClO_4)_2$, and $NaHCO_3$ were monitored as a function of small aliquots of $HClO_4$. The observation, shown in Figure 8, is that once equilibrium is attained the maximum absorbance changes occur at 600 nm, reflecting (as expected) the change in BCP anion concentration. Control experiments indicate that the various buffer and indicator equilibria alone are established rapidly. However, in the presence of $NaHCO_3$ spectra changes do depend upon time since the dehydration process takes some 5–10 s to attain equilibrium. In order to evaluate the characteristics of the spectral changes during the course of dehydration, a stopped-flow procedure was employed in which absorbance vs. time points were taken at various wavelengths. The result, shown in Figure 9, indicates that where two solutions containing BCP, Zn^{2+}, and HCO_3^- are rapidly combined, the maximum absorbance changes

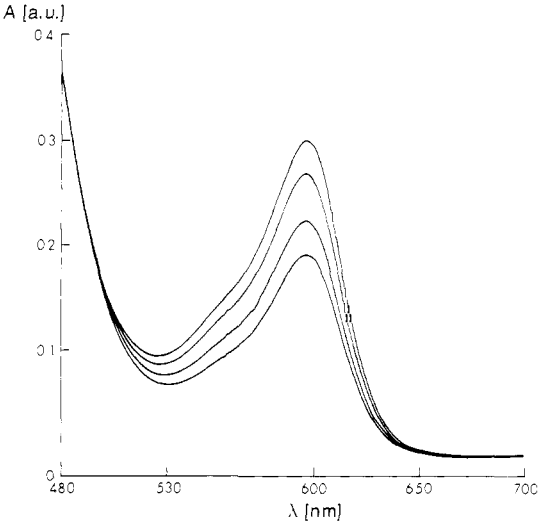

Figure 8. Visible absorption spectra showing the equilibrium situation for buffered solutions of BCP as a function of added 1 μL aliquots of 0.1 M $HClO_4$: 2.5×10^{-2} M HEPES, 2.5×10^{-4} M BCP, 2.5×10^{-4} M $Zn(ClO_4)$, $[NaHCO_3]$ initially 2.5×10^{-3} M, 0.2 M $NaClO_4$, 80% $EtOH/H_2O$.

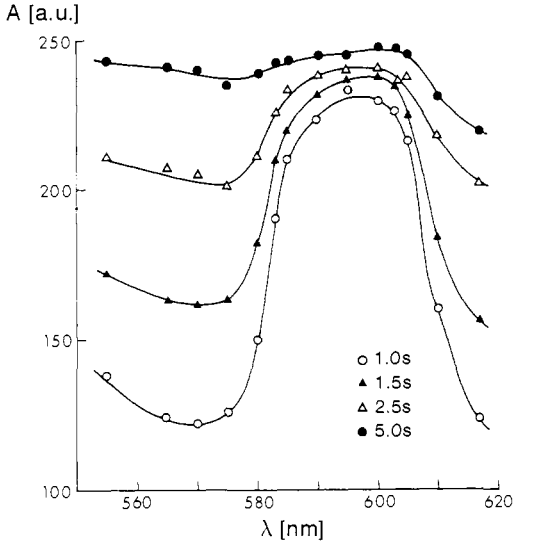

Figure 9. Transient absorption spectra of a buffered solution (same initial conditions as in Figure 8) as a function of time.

(23) Equation 11 represents an example of a reversible enzyme catalyzed reaction in which a substrate is involved on both sides of the equation first discussed by Haldane

$$E + A \underset{k_{-1}}{\overset{k_1}{\rightleftarrows}} EA \underset{k_{-2}}{\overset{k_2}{\rightleftarrows}} EX \underset{k_{-3}}{\overset{k_3}{\rightleftarrows}} E + X$$

(Haldane, J. B. S. "Enzymes"; Longmans, Green and Co.: London, 1930; p 81). While study of a reversible reaction of this type will not permit evaluation of the individual rate constants without the use of special methods, in the limiting cases where pure A (in this case HCO_3^-) is used, the initial rate of the reaction can be shown to be

$$V_i = \frac{V_A[A]}{K_A + [A]}$$

where

$$V_A = \frac{k_2k_3}{k_2 + k_{-2} + k_3}[E_0]$$

$$K_A = \frac{k_{-1}k_{-2} + k_{-1}k_3 + k_2k_3}{k_{-3}(k_{-1} + k_2 + k_3)}$$

For a discussion of this see: Laidler, K. J.; Bunting, P. S. "The Chemical Kinetics of Enzyme Action", 2nd ed.; Oxford University Press: London, 1973; p 81.

Scheme II[a]

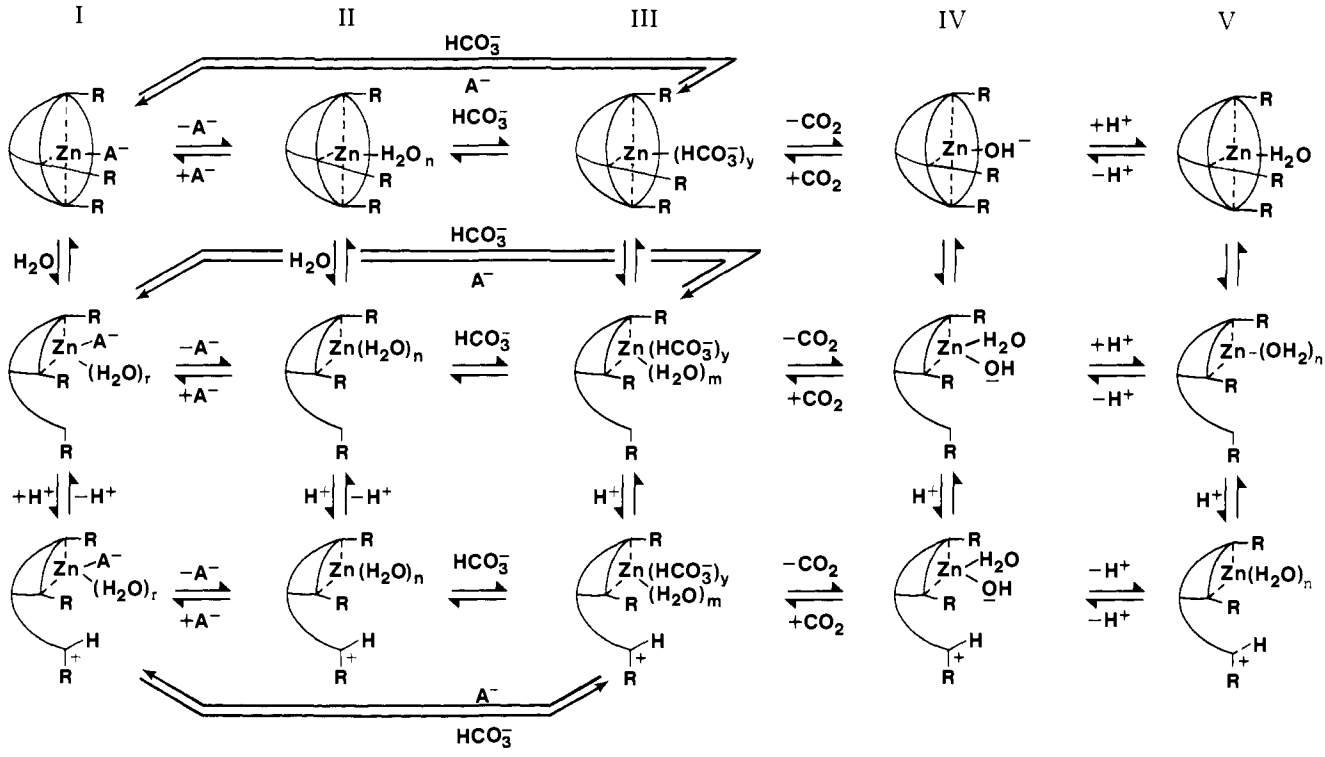

[a] Metal charges omitted for simplicity.

occur not at 600 nm, but at ~570 nm. Such indicates that a transient complex between BCP, Zn^{2+}, and HCO_3^- is formed having different spectral characteristics than BCP and Zn^{2+} alone. Since it is known that BCP can complex with M^{X+} ions,[24] it is not unexpected that such complexes will be perturbed by other species in solution, such as our ligands[25] and various anions (HCO_3^-) capable of associating with M^{2+}. These observations preclude the exact evaluation of k_f under the conditions employed for the kinetic studies since the buffer factor of the indicator is therefore dependent upon the presence of HCO_3^-. It should be stated, however, that k_{obsd} can be assessed since it is a reflection of all processes which respond to the changing [HCO_3^-] as equilibrium is attained. This is verified by the fact that k_{obsd} is independent of λ. Furthermore, since control experiments establish that Zn^{2+} or ligand alone do not increase k_{obsd} over the blank value nor is the value of k_{obsd} dependent upon [BCP],[25] it is the cooperative interaction of ligand and Zn^{2+} which leads to a faster reaction.

Although we can confidently claim that the association of these ligands with Zn^{2+} can provide quite respectable catalysts for catalyzing $HCO_3^- \rightleftarrows CO_2$ equilibration and do approximate many of the features of the active site, they fall far short of approaching the rates afforded by CA and therefore must be imperfect. It is best they be considered as catalytic entities in their own right and to avoid strong parallels with the enzyme although certain implications are justified.

Since we have presented evidence (vide supra) that indicates that at the pHs and anionic conditions where the catalysts show their maximal activities in promoting the $HCO_3^- \rightleftarrows CO_2$ equilibration, the complexes are undergoing rapid ligand exchange, we must consider that several forms of the complex are present in solution in a dynamic equilibrium. For the sake of simplicity we have presented only three of these forms in each column of Scheme II. Although this is not meant to eliminate other forms that may be catalytically viable, the major distinctions in progressing down a given column (e.g., column II) is in the state of coordination number of the Zn^{2+} and number of associated solvent molecules as well as the state of protonation of the ligand.

Disassociation of an imidazole not only increases accessibility of species from the solution (H_2O, A^-, HCO_3^-, or CO_2) to the Zn^{2+} but could provide a closely situated base to assist in proton transfer which must accompany, precede, or succeed the catalytic event.[18] When introduced into solution, HCO_3^- can associate with any one (or all) of the coordinated $L{\cdot}Zn^{2+}$ species to form a set of ternary complexes (column III) from which the expulsion of CO_2 occurs. Although we have no direct evidence for its involvement from this study, we favor (as do others[1,2,4a-c,h]) formation of a $L{\cdot}Zn^{2+}{-}OH^-$ (column IV) after CO_2 elimination which subsequently undergoes reprotonation to yield a metal bound H_2O (column V).

The effect of inhibitory anions can be viewed as an overall perturbation of the equilibrium toward the $L{\cdot}Zn^{2+}A^-$ ternary complexes shown in column I. Associated anions will not only electrostatically perturb the acid–base equilibria of the ligand and $Zn^{2+}{-}OH_2$, but resist displacement by HCO_3^-, both factors leading

(24) (a) For a general account of the indicator usages of BCP see: "Indicators"; Bishop, E., Ed.; Pergamon: Braunschweig, 1972; pp 106–107. (b) Wawrzyczek, W.; Wiśniewski, W. *Z. Anal. Chem.* **1964**, *203*, 329–334.

(25) (a) It has been noted that BCP exhibits color changes in the presence of a variety of N-containing alkaloids: Thomis, G. N.; Kotionis, A. Z. *Anal. Chim. Acta* **1957**, *16*, 201–206. (b) We also observe a color change when ligand **5** is introduced into solutions containing BCP. Furthermore, if the [BCP] < 2.5×10^{-4} M, a visible precipitation of **5** (but not the other ligands) occurs after a few minutes. This is not the case with **1c** or **4a,b**. [BCP] was therefore kept > 2.5×10^{-4} M and k_{obsd} is independent of further increases in concentration. Such suggests an association of **5** and BCP in these solutions so that the species involved in the catalytic medium might well be a rather complex aggregate. Nevertheless, on the basis of the control experiments it is the ligand and Zn^{2+} together which are the critical components of the mixture. While the indicator does play some undefined (and perhaps not completely innocent) role which complicates the system, it alone or in the absence of either Zn^{2+} or ligand cannot be responsible for the observed catalysis. We have attempted to use other indicators to obviate this problem, but such has proved fruitless for either solubility reasons or because the 80% $EtOH/H_2O$ perturbs the acid–base behavior of the indicators to be outside the pH range used for the study. (c) It might be considered that one way to circumvent the problem of $HCO_3^-{-}M^{2+}{-}BCP$ interactions which perturb the buffer factor would be to evaluate k_r from the direction of CO_2 hydration. We have conducted these experiments and find that indeed k_r does increase with increasing [catalyst] and [CO_2]. However, since K_{eq} at pH 6.4–6.5 is ~8–10, k_r varies from ~0.06–0.2 s^{-1} for 5×10^{-4} M **4a**·Zn^{2+} when $[CO_2]_i$ ranges from 2×10^{-3} M–10×10^{-3} M. Since the precision of k_r is only ±0.03 s^{-1}, a large uncertainty in the values is present. If the catalysts were more active, such an experiment would be feasible, but for the present molecules it is not.

to a reduced catalytic viability of the complex.

Conclusions

(1) Although each ligand (**1c**, **4a**, and **5**) associates strongly with Zn^{2+}, the complexes are probably not exclusively tricoordinated under conditions where catalysis is evident since NMR studies show a dynamic behavior.

(2) The visible absorption spectra of **5**·Co(II)–Cl_x show formation of two different tetrahedral complexes as a function of pH. The spectrum is also anion dependent, indicating that these associate with the metal to form tetrahedral or 5-coordinate complexes. The **4a**·Co(II) absorption spectrum shows only a small amount of tetrahedral species.

(3) Catalytically the Zn^{2+} complexes of **1c**, **4a**, and **5** accelerate the attainment of $HCO_3^- \rightleftarrows CO_2$ equilibrium. The maximum catalytic rate constants are 900 M^{-1} s^{-1}, 1500 M^{-1} s^{-1}, and 2700 M^{-1} s^{-1}, respectively, and show that accessibility of $HCO_3^-(CO_2)$ to the Zn^{2+} and a hydrophobic metal environment are both important features for catalysis. Anions inhibit the reaction by associating with the metal which prevents access of the reactants.

(4) The rate of attainment of equilibrium increases as a function of $[HCO_3^-]$ in a manner indicative of a saturation behavior.

(5) Initial rate measurements to determine the rate constant for HCO_3^- cannot be made due to the inability to obtain the buffer factors under the experimental conditions.

Acknowledgment. We gratefully acknowledge the University of Alberta, Natural Sciences and Engineering Research Council of Canada, and the Petroleum Research Fund, administered by the American Chemical Society, for partial financial support of this work. In addition, we are grateful to the Alberta Heritage Medical Research Foundation for funds enabling purchase of the stopped-flow instrumentation and to Prof. H. B. Dunford and Dr. J. M. Buschek for stimulating conversations.

Registry No. 4a, 89210-50-4; **4b**, 89210-51-5; **5**, 89210-52-6; 6, 84802-87-9; CA, 9001-03-0; *N*-(dimethoxymethyl)-4,5-diisopropylimidazole, 74483-01-5; chlorobis(*N*-dimethoxymethyl)-4,5-diisopropyl-2-imidazolyl)phosphine, 89210-53-7; *N*-(diethoxymethyl)-4,5-di-*n*-propylimidazole, 89210-54-8; 4,5-di-*n*-propylimidazole, 24363-69-7; bicarbonate, 71-52-3.

Communications to the Editor

Mills–Nixon Effect, a Resolution: Clear Evidence for No Significant π-Bond Localization in Small Ring Annelated Aromatics. The Synthesis and Diatropicity of Cyclobutane Annelated Dihydropyrenes[1]

Reginald H. Mitchell,* Paul D. Slowey, Toshihiro Kamada, Richard Vaughan Williams, and Peter J. Garratt[2]

Department of Chemistry, University of Victoria Victoria, British Columbia, Canada V8W 2Y2

Received September 22, 1983

Mills and Nixon postulated over 50 years ago[3] that the strain of fusing a five-membered ring onto a benzene ring caused partial π-bond localization in the aromatic system. This hypothesis initiated many synthetic and spectroscopic papers attempting to prove or disprove the effect.[4] The problem was given new impetus by theoretical predictions,[5] and this led to the synthesis of a variety of benzocyclopropenes[4e] and benzocyclobutenes,[4g] including bis- and tris-annelated derivatives,[4g,h,l] annelated heterocyclic aromatics,[4f,j] and annelated naphthalenes.[4i,k] These have been subject of considerable analysis, for example, by ^1H and ^{13}C NMR, both coupling constants and chemical shifts,[4b,c,g,i,l] by ultraviolet spectroscopy,[4g,i,l] and by X-ray crystallography,[4d,h,k] and have also been the subject of theoretical calculations.[4c]

Although changes in both the physical and chemical properties of such compounds were observed and have been explained on the basis of rehybridization,[6] no experiment has yet shown whether a measurable degree of double bond localization occurs. This is in part due to the fact that a molecule such as benzene or naphthalene is not very readily probed in terms of π-electron delocalization.

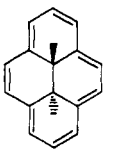

1

Dimethyldihydropyrene **1** on the other hand is.[7] The chemical shift of the internal methyl groups of **1** (δ −4.25) is very sensitive to the degree of delocalization in the macrocyclic ring, and we have shown[8] that the chemical shift shielding (Δδ) of the internal methyl protons of **1** is related to the average deviation in π-SCF bond order (Δr)[9] by eq 1. While this equation was derived by

$$\Delta\delta = 5.533 - 0.02752\Delta r \quad (1)$$

study of a number of benzannelated annulenes, we have conclusively shown[8] that the anisotropy effects of the annelating rings are small relative to effects caused by changes in delocalization. Moreover, dihydropyrenes with only external alkyl groups or saturated annelated rings would not be expected to cause sub-

(1) Annelated annulenes Part 10. For part 9, see: Mitchell, R. H.; Williams, R. V.; Mahadevan, R.; Lai, Y. H.; Dingle, T. W. *J. Org. Chem.* **1982**, *47*, 5210.

(2) Department of Chemistry, University College London, London WC1H 0AJ, U.K.

(3) Mills, W. H.; Nixon, I. G. *J. Chem. Soc.* **1930**, 2510.

(4) See, for example, and also the references quoted therein: (a) Badger, G. M. *Q. Rev. Chem. Soc.* **1951**, *5*, 147. (b) Cooper, M. A.; Manatt, S. L. *J. Am. Chem. Soc.* **1970**, *92*, 1605. (c) Cheung, C. S.; Cooper, M. A.; Manatt, S. L. *Tetrahedron* **1971**, *27*, 701. (d) Billups, W. E.; Chow, W. Y.; Leavell, K. H.; Lewis, E. S.; Margrave, J. L.; Sass, R. L.; Shieh, J. J.; Werners, P. G.; Wood, J. L. *J. Am. Chem. Soc.* **1973**, *95*, 7878. (e) Halton, B. *Chem. Rev.* **1973**, *73*, 113. (f) Garratt, P. J.; Nicolaides, D. N. *J. Org. Chem.* **1974**, *39*, 2222. (g) Thummel, R. P.; Nutakul, W. *Ibid.* **1977**, *42*, 300. (h) Korp, J. D.; Thummel, R. P.; Bernal, I. *Tetrahedron* **1977**, *33*, 3069. (i) Thummel, R. P.; Nutakul, W. *J. Am. Chem. Soc.* **1978**, *100*, 6171. (j) Thummel, R. P.; Kohli, D. K. *Tetrahedron Lett.* **1979**, 143. (k) Korp, J. D.; Bernal, I. *J. Am. Chem. Soc.* **1979**, *101*, 4273. (l) Davalian, D.; Garratt, P. J.; Koller, W.; Mansuri, M. M. *J. Org. Chem.* **1980**, *45*, 4183. (m) Davalian, D. Ph.D. Thesis, University of London, London, G.B., July 1976.

(5) Longuet-Higgins, H. C.; Coulson, C. A. *Trans. Faraday Soc.* **1946**, *42*, 756.

(6) Streitweiser, A.; Ziegler, G. R.; Mowery, P. C.; Lewis, A.; Lawler, R. G. *J. Am. Chem. Soc.* **1968**, *90*, 1357. Finnegan, R. A. *J. Org. Chem.* **1965**, *30*, 1333. Taylor, R.; Wright, G. F.; Holmes A. J. *J. Chem. Soc. B* **1967**, 780; **1968**, 1559; **1971**, 536. Taylor, R.; David, M. P.; McOmie, J. F. W. *Ibid.* **1972**, 162. Riecke, R. D.; Rich, W. E.; Ridgeway, T. H. *J. Am. Chem. Soc.* **1971**, *93*, 1962. Riecke, R. D.; Rich, W. E. *Ibid.* **1972**, *92*, 7349. Bassindale, A. R.; Eaborn, C.; Walton, D. M. R. *J. Chem. Soc. B* **1969**, 12.

(7) Mitchell, R. H.; Carruthers, R. J.; Mazuch, L.; Dingle, T. W. *J. Aam. Chem. Soc.* **1982**, *104*, 2544.

(8) Mitchell, R. H.; Williams, R. V.; Mahadevan, R.; Lai, Y. H.; Dingle, T. W. *J. Am. Chem. Soc.* **1982**, *104*, 2571.

(9) Δr is defined[8] as $\Delta r = (\sum m|(P_\mu - 642)|)/m$ where $P_\mu = \pi$-SCF bond order x 10^3 of the μth bond, and m is the number of bonds in the macrocycle (= 14 in **1**).

0002-7863/84/1506-2431$01.50/0